Journal of Alloys and Compounds 520 (2012) 140–145

Contents lists available at SciVerse ScienceDirect

Journal of Alloys and Compounds

journal homepage: www.elsevier.com/locate/jallcom

Microstructural and optoelectronic properties of diluted magnetic semiconducting $Cd_{1-x}Fe_xS$ nanocrystalline films

M. El-Hagary[a,b,*], E.R. Shaaban[c], M. Emam-Ismail[a,d], S. Althoyaib[a]

[a] Physics department, College of Science, Qassim University, P. O. 6644, 5145 Buryadh, Saudi Arabia
[b] Physics Department, Faculty of Science, Helwan University, 11792 Helwan, Cairo, Egypt
[c] Physics Department, Faculty of Science, Al-Azhar University, Assuit, Egypt
[d] Physics Department, Faculty of Science, Ain Shams University, 11566 Abbassia, Cairo, Egypt

ARTICLE INFO

Article history:
Received 27 November 2011
Received in revised form
26 December 2011
Accepted 30 December 2011
Available online 8 January 2012

Keywords:
Nanomaterial
Diluted magnetic semiconductors
Microstructure properties
Optical properties
Single oscillator parameters

ABSTRACT

We report the preparation of electron beam evaporated Fe-doped CdS nanocrystalline thin films ($Cd_{1-x}Fe_xS$) with different doping concentrations ($x = 0.002$, 0.05, 0.1, 0.15 and 0.2) and characterization of their microstructural and optoelectronic properties. The structural properties investigated by X-ray diffraction revealed cubic zincblende CdS type structure and a decrease of lattice parameter with Fe doping confirming incorporation of Fe in Cd atom positions. The crystallite size of the films was found to vary from 33 to 20 nm with increasing Fe content. The elemental chemical stoichiometric was studied by energy dispersive X-ray analysis. The optical characterization of the films has been carried out from spectral transmittance and reflectance obtained by double beam spectrophotometer in the wavelength range from 190 to 2500 nm. The refractive index and extinction coefficient have been found to increase with increasing Fe content. The increase in the refractive index has been explained on the basis of polarizability. Dispersion of refractive index has been analyzed in terms of the Wemple–DiDomenico single oscillator model. The oscillator parameters; the single oscillator energy E_0, the dispersion energy E_d, the static refractive index n_0, average interband oscillator wavelength λ_0, and the average oscillator strength S_0 were estimated. It was further found that the optical energy gap decreases from 2.470 eV to 2.338 eV with increasing Fe content from $x = 0.002$ to $x = 0.2$ which is suggested to be related to the *sp–d* exchange interaction with the Fe^{2+} magnetic moments.

1. Introduction

Diluted magnetic semiconductors (DMS) of III–V or II–VI are a new class of materials where semiconductors doped with magnetic impurities [1,2]. Diluted magnetic semiconductors are expected to play an important role in the future of the electronic science because of the combine elements of semiconductors (charge) and magnetism (spin) into a single material, known as spintronic. The existence of the strong exchange interactions between *s–p* band electrons and *d*-electrons associated with magnetic ion leads to useful optical and electrical properties [3,4]. Recently, DMS have attracted extensive research interests due to their unique magnetic and optical properties and potential applications [5,6].

Among these materials Fe doped II–VI semiconductors in the form of thin film have been studied [7–9]. The homogeneity of dopant incorporation as well as the precise control of the film growth may be responsible for the change in the physical properties of the films obtained by the different groups. However, studies of the optical properties on $Cd_{1-x}Fe_xS$ are very few [10]. It is well known that the determination of the optical parameters is expected to extend the available physical information which is essential for design the optical, magneto-optical devices and magnetic sensors.

Therefore the objective of this investigation is to report on the nanostructural and optical properties of the diluted magnetic semiconductors $Cd_{1-x}Fe_xS$ ($0.002 \leq x \leq 0.2$) thin films deposited on glass substrate by electron beam evaporation technique upon the effect of variations of Fe concentration into the CdS matrix. Moreover, the room temperature reflectance and transmittance data are carefully analyzed to identify the refractive index and single oscillator parameters such as, oscillator energy, oscillator strength, dispersion energy, zero-frequency dielectric constant and zero frequency refractive index.

2. Experimental details

Polycrystalline samples of $Cd_{1-x}Fe_xS$ with different Fe concentration ($x = 0.002$, 0.05, 0.1, 0.15 and 0.2) were prepared by solid state reaction method. Stoichiometric

* Corresponding author at: Physics Department, College of Science, Qassim University, P. O. 6644, 5145 Buryadh, Saudi Arabia. Tel.: +966 6 3800050 4092; fax: +966 6 3801581.
E-mail addresses: magelhagary@yahoo.com, magelhagary@gmail.com (M. El-Hagary).

0925-8388/$ – see front matter © 2012 Elsevier B.V. All rights reserved.
doi:10.1016/j.jallcom.2011.12.160

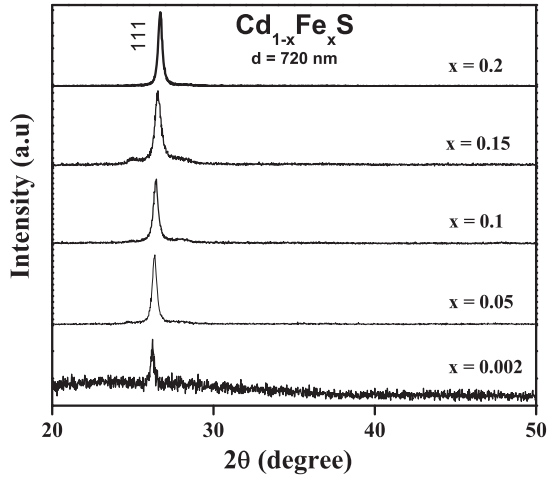

Fig. 1. XRD patterns of $Cd_{1-x}Fe_xS$ thin films with different Fe composition (x = 0.002, 0.05, 0.1, 0.15 and 0.2).

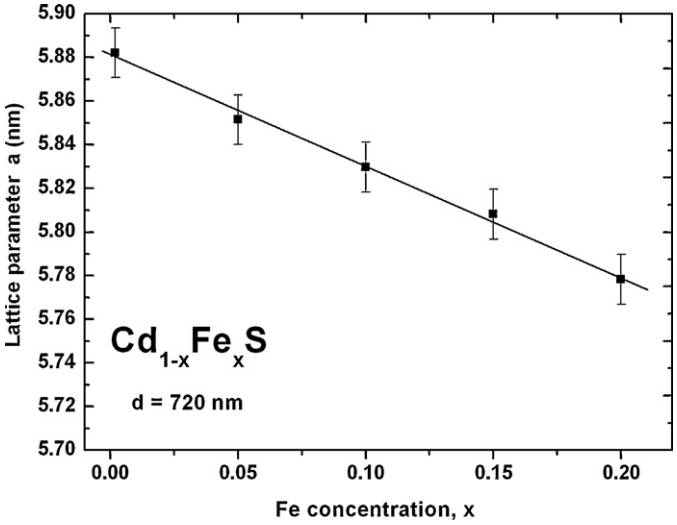

Fig. 2. Dependence of the lattice parameter with Fe concentration of $Cd_{1-x}Fe_xS$ thin films.

amounts of high-purity (99.999%) analytical grade CdS and FeS powders (Sigma–Aldrich Co., USA) were mixed by grinding in a ball mortar for about 10 h. Direct evaporation of the mixture in powder form resulted in sputtering of the powder when the boat is heated. Thus, the mixed powders were pressed into a disk-shape pellet. Thin films of $Cd_{1-x}Fe_xS$ with various Fe concentration (x = 0.002, 0.05, 0.1, 0.15 and 0.2) were prepared by electron beam evaporation using high vacuum coating unit type Edward Auto 306. The system was pumped to a pressure of 5×10^{-6} Pa. The pellets of $Cd_{1-x}Fe_xS$ samples with $0.002 \leq x \leq 0.2$ were heated in a vacuum chamber with the electron gun in order to degas the material before evaporation process. The films were deposited on amorphous glass substrates (25 mm × 25 mm) maintained at room temperature (300 K). The substrates were carefully cleaned by using acetone and distilled water. The thickness of the films was kept to be constant at 720 nm (±10 nm) for all composition studies. The substrates were rotated during the deposition. The source to the substrate distance was about 20 cm to get a deposition rate of 2 nm/s. The thickness of the films and the rates of evaporation were monitored with a quartz crystal thickness monitor attached to the vacuum system. For more details about the applied methodology see, e.g. [11,12].

The structure and phase purity of the samples and as-deposited films were checked at room temperature by means of X-ray powder diffraction (XRD) Shimadzu Diffractometer XRD 6000, Japan, with Cu-Kα1 radiation (λ = 1.54056 Å). The data were collected by step-scan modes in a θ–2θ range between 10° and 80° with step-size of 0.02° and step time of 0.6 s. Pure Silicon ~Si 99.9999% was used as an internal standard. The elemental composition of the films was analyzed by using energy dispersive X-ray spectrometer unit (EDXS) interfaced with a scanning electron microscope, SEM (JOEL XL) operating an accelerating voltage of 30 kV. The relative error of determining the indicated elements does not exceed 5%.

Optical characterization of the films has been preformed from spectral transmittance and reflectance, which were obtained through JASCO V-670 double beam spectrophotometer. The measurements have been performed in the wavelength range from 190 to 2500 nm. The transmittance and reflectance measurements were taken at normal incident.

3. Results and discussion

3.1. Structural properties

Fig. 1 shows the X-ray diffraction patterns (XRD) of the as deposited $Cd_{1-x}Fe_xS$ thin films with different Fe doping concentration (x = 0.002, 0.05, 0.1, 0.15 and 0.2). Comparing the diffraction peaks position with the data from JCPDS international diffraction database. It is found that these peaks occurred at 26.22°, 26.36°, 26.46°, 26.56°, and 26.70° (for thin films with different Fe doping concentration x = 0.002, 0.05, 0.1, 0.15 and 0.2, respectively) correspond to (1 1 1) can be distinctly assigned to cubic zincblende CdS type structure (JCPDS No. 75-0581). Furthermore, all the films exhibit preferential orientation along (1 1 1) plane. It is known that CdS based compounds have a stable hexagonal wurtzite phase [10,13] and a metastable zincblende cubic phase [14]. It is also observed that the position of the diffraction peak (1 1 1) is shifted systematically towards higher values of the diffraction angle 2θ by increasing Fe concentration indicating the changes in the lattice parameter due to the presence of the tensile strain in the host on incorporation of the dopant ions into the basic cell in the grown films. The shifting of the peak position is also confirms that the Fe is replaced in Cd atom positions.

The lattice parameter a of the unit cell of the investigated films were determined according to the standard relation of the cubic system:

$$\frac{1}{d_{hkl}^2} = \frac{h^2 + k^2 + l^2}{a^2} \quad (1)$$

The dependence between the lattice constant with compositions, x is illustrated in Fig. 2 and list in Table 1. Apparently, the lattice parameter decreases linearly with increasing x which agrees well with Vegard's law and confirms the formation of substitutional solid solution of the $Cd_{1-x}Fe_xS$. The obtained lattice parameter of the pure CdS film is in good agreement with those reported in the literature [14]. A relative decrease in the lattice parameter is due to the difference between the ionic radius of Cd^{2+} (0.97 Å) and ionic radius of Fe^{2+} (0.76 Å) indicating a local contraction of the lattice, see Table 1.

It is also clear from Fig. 1 that all the diffraction peaks exhibit a significant line broadening which is attributed to both particles size and crystal defects indicating the nanostructure nature of the films.

Table 1
The microstructural data of nanocryatalline $Cd_{1-x}Fe_xS$ thin films with different compositions.

x	2θ (°)	a (Å)	V (Å^3)	FWHM × 10^{-3} (Rad)	D (nm)	$\varepsilon \times 10^{-3}$	$\delta \times 10^{16}$ (Lin/m^2)
0.002	26.22	5.88215(3)	203.520	4.286	33.21	4.601	0.906
0.05	26.36	5.85145(4)	200.350	5.358	26.58	5.720	1.415
0.1	26.46	5.82973(3)	198.127	5.497	25.91	5.846	1.489
0.15	26.56	5.80817(3)	195.938	6.806	20.92	7.209	2.284
0.2	26.70	5.77827(4)	192.927	7.103	20.06	7.483	2.485

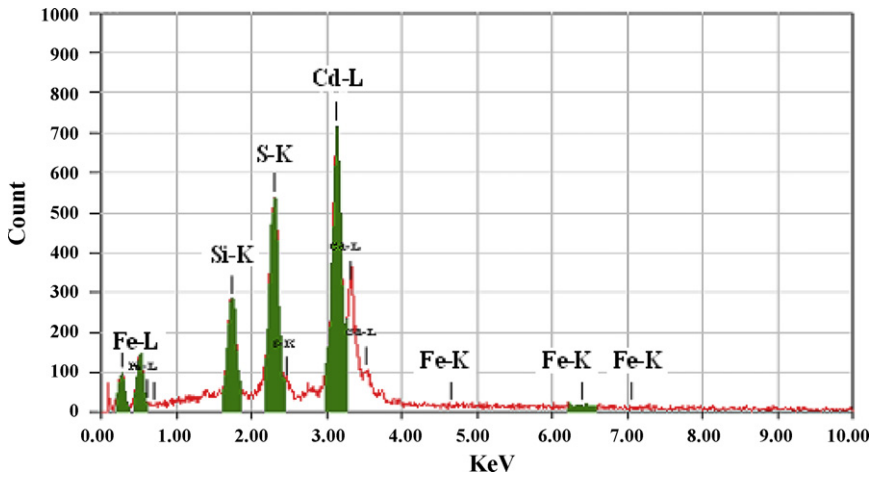

Fig. 3. Typical EDXS spectra of nanocrystalline $Cd_{0.9}Fe_{0.1}S$ film.

The microstructural parameters like grain size, crystal strain and dislocation density have been calculated. The average grain sizes (D) of $Cd_{1-x}Fe_xS$ films were calculated from the XRD peaks using Scherrer's formula [15],

$$D = \frac{k'\lambda}{\beta \cos\theta} \tag{2}$$

where D is the crystallite size, λ is the wavelength of the X-ray used, β is the full width at half maximum (FWHM) of diffraction peak in radians, θ is the corresponding Bragg angle and k' is a constant approximately equal to 0.9. The lattice strain, ε was calculated by using the Scherrer's relation [15]

$$\varepsilon = \frac{\beta}{4\tan\theta} \tag{3}$$

The dislocation density (δ), defined as the length of dislocation lines per unit volume of the crystal, was evaluated from the formula [16]:

$$\delta = \frac{1}{D^2} \tag{4}$$

The microstructural parameters of the investigated films are summarized in Table 1. The average crystallite size (D) of as-deposited films of all compositions of $Cd_{1-x}Fe_xS$ is observed to vary from 20 to 33 nm confirming the nanocrystalline nature of $Cd_{1-x}Fe_xS$ films. As can be seen the increase of Fe content in the CdS matrix increases the FWHM which results in improve the crystallinity and decrease in grain size of the films. Nevertheless, both the crystal strain and dislocation density increase with increasing of the Fe concentration.

3.2. Compositional analysis

A typical energy dispersive X-ray spectrum (EDXS) of as-deposited film of $Cd_{0.9}Fe_{0.1}S$ is shown in Fig. 3. The compositional analysis data for the as-deposited film confirm the presence of Cd, Fe, and S elements with contribution of extra peak of Si from glass substrate. The ratio of Cd:Fe:S is observed to be about 45.10 at.%:4.85 at.%:50.1 at.% which indicated that the composition was nearly stoichiometric. Similarly, stoichiometry of all grown films has been also observed.

3.3. Optical properties

3.3.1. Determination of optical constants

The absolute value of $T(\lambda)$ and $R(\lambda)$ were calculated according to the following equation [17,18]:

$$T = \left(\frac{I_{ft}}{I_g}\right)(1 - R_g) \tag{5}$$

where I_{ft} and I_g are the intensities of light passing through the film-glass substrate and the reference glass substrate, respectively.

$$R = \left(\frac{I_{ft}}{I_{A1}}\right) R_{A1}\left[1 + (1 - R_g)^2\right] - T^2 R_g \tag{6}$$

I_{fr}, I_{Al} are the intensities of light reflected from the sample and that from the reference mirror, respectively and R_g being the reflectance of glass. The variation of absolute value of $T(\lambda)$ and $R(\lambda)$ against wavelength λ for the as deposited films of $Cd_{1-x}Fe_xS$ with different Fe content is shown in Fig. 4. All the samples show a sharp fall in transmittance at the fundamental absorption band edge. This sharp edge corresponds to electron excitation from the valance band to conduction band and interrelated to the nature and value

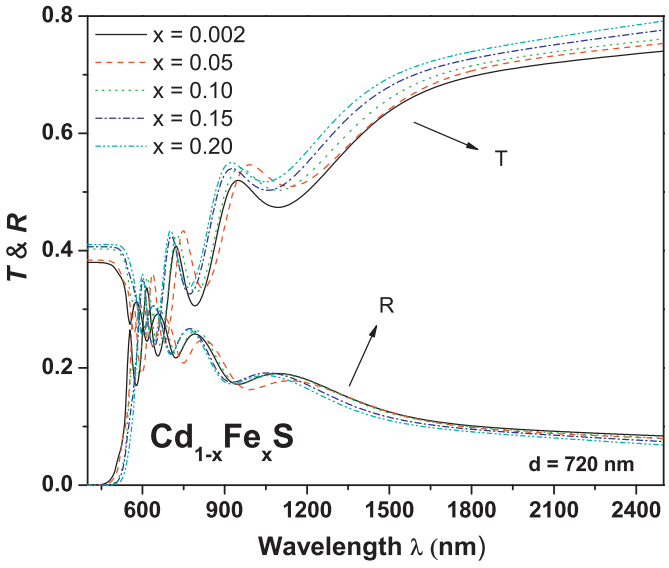

Fig. 4. The variation of absolute value of $T(\lambda)$ and $R(\lambda)$ against wavelength λ for the as deposited films of $Cd_{1-x}Fe_xS$ with different Fe content.

of the optical band gap. A remarkable shift of absorption edge towards higher wavelengths (red shift) with increasing Fe content is observed. According to the fundamental Kramers–Kroning relations, the red shift in the spectral distribution must necessarily give an increased refractive index value (see later).

For determination the optical constants, refractive index n and extinction coefficient k, a method comprise a search technique based on minimizing $(\Delta T)^2$ and $(\Delta R)^2$ simultaneously has been used, where

$$(\Delta R)^2 = \left|R_{calc}(n, k, d, \lambda) - R_{exp}\right|^2 \quad (7)$$

$$(\Delta T)^2 = \left|T_{calc}(n, k, d, \lambda) - T_{exp}\right|^2 \quad (8)$$

where T_{exp} and R_{exp} are the experimentally determined values of T and R, respectively, and T_{calc} and R_{calc} are the calculated values of T and R, using Murmann's exact equation [19]. The adapted computation steps are as follows:

- The measured transmittance, T_{exp}, measured reflectance R_{exp}, film thickness; d and the refractive index of substrate n_s are entered.
- The film thickness d is an important parameter in the accurate determination of the optical constant. Therefore different methods have been used for determination of the thickness of the deposited films. Such thickness has been firstly estimated in situ by using a quartz crystal thickness monitor pre-calibrated interferometrically by using multiple beams Fizeau fringes at reflection [20].
- Ranges of refractive index, n and ranges of the extinction coefficient, k within which the optimal solution is expected. The desired accuracy in n and k are putted as increments in n and k, respectively.
- Using the Murmann's equation [19], both T_{calc} and R_{calc} are calculated throughout the whole ranges.
- In each step the variances $(\Delta T)^2$ and $(\Delta R)^2$ are calculated and compared, to seek their simultaneous minimization. The corresponding values of n and k represent the solution. During the iteration, in some small regions of the spectrum the solutions may be missing. The missing part can be interpolated by using the program origin version 7 (OriginLab Corp.).

The dispersion of the refractive index (n) and extinction coefficient (k) for $Cd_{1-x}Fe_xS$ films with different compositions (x = 0.002, 0.05, 0.1, 0.15 and 0.2) are shown in Fig. 5(a) and (b). It can be seen that both the refractive index and the extinction coefficient increases with increasing the Fe concentration. The increase in refractive index with increasing Fe content may be attributed to the increase in the polarizability. The atomic radii of Cd, Fe and S are 1.71 Å, 1.72 Å and 1.09 Å, respectively [21]. The larger atomic radius of the atom, the larger will be its polarizability. Therefore, such dependence of the refractive index on the Fe content of the investigated films can be explained on the basis of Lorentz–Lorenz equation in which a direct proportion between the polarizability and refractive index is established [21]. Thus, substituting of more polarisable Fe atoms by less polarisable Cd may lead to an increase of refractive index.

3.3.2. Determination of the single oscillator parameters

The spectral dependence data of the refractive index dispersion of the as deposited $Cd_{1-x}Fe_xS$ thin films with different Fe content (x = 0.002, 0.05, 0.1, 0.15 and 0.2) can be evaluated according to the single-effective-oscillator model proposed by Wemple–DiDomenico (WDD) [22]. The model suggests that the

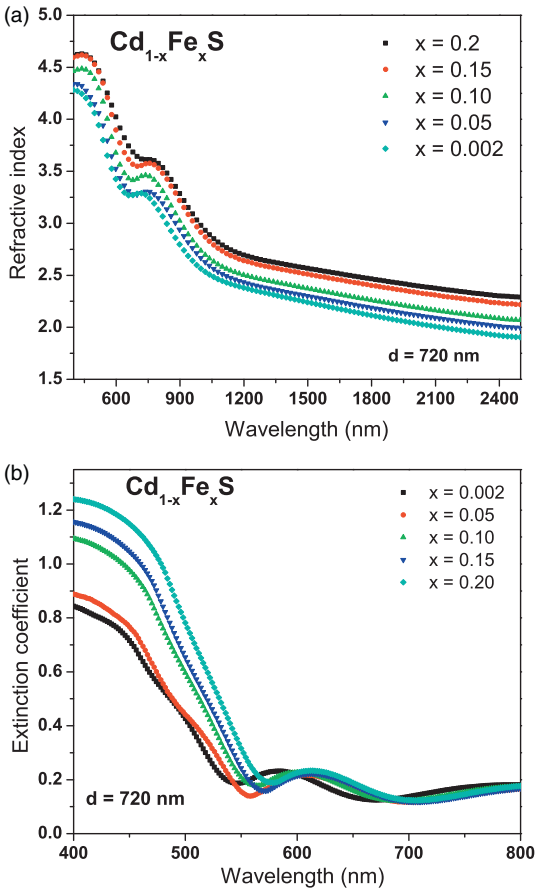

Fig. 5. The dispersion of the (a) refractive index (n) and (b) extinction coefficient (k) for $Cd_{1-x}Fe_xS$ films with different compositions (x = 0.002, 0.05, 0.1, 0.15 and 0.2).

refractive index, n, of the films could be correlated to the oscillator energy, E_0, and the dispersion energy, E_d, by the following formula:

$$n^2 = 1 + \frac{E_0 E_d}{E_0^2 - (h\nu)^2} \quad (9)$$

where $(h\nu)$ is the photon energy and E_0, E_d are single-oscillator constants.

Shown in Fig. 6 is the optical dispersion behavior, $(n^2-1)^{-1}$ against $(h\nu)^2$, of the investigated nanocrystalline $Cd_{1-x}Fe_xS$ thin films with different Fe content. The oscillator parameters E_0 and E_d were determined by fitting a straight line to the points. The slope of the linear relationship represents the $(E_0E_d)^{-1}$ and intercept with the vertical axis equal to (E_0/E_d). The values obtained of dispersion parameters, E_0 and E_d for as deposited $Cd_{1-x}Fe_xS$ films are listed in Table 2. Furthermore, the oscillator energy E_0 (or the effective oscillator energy) can be directly correlated with the optical energy gap E_g^{opt} by an empirical formula, $E_0 = 2 \times E_g^{opt}$, as was found by Tanaka [23]. It was observed that the values of $E_g^{opt(WDD)}$ are almost in agreement with that obtained from the Tauc's extrapolation model [24], see Table 2. Also, the dispersion energy (or the oscillator strength) follows a simple empirical relationship: $E_d = \beta N_c Z_a N_e$ where β is a constant having two values of either 0.26 ± 0.03 eV for ionic materials or 0.37 ± 0.04 eV for covalent materials [22], N_c is the coordination number of the cation nearest neighbour to the anion ($\cong$4 for $Cd_{1-x}Fe_xS$), Z_a is the formal chemical valency of the anion and N_e is the total number of valence electron (core electrons are excluded) per anion which is calculated from the above empirical formula, see Table 2. It is found that N_e increases with the increase in the Fe concentration, x. Obviously, it is found that E_0 decreases with increasing x while, E_d increases. The decrease in the oscillator

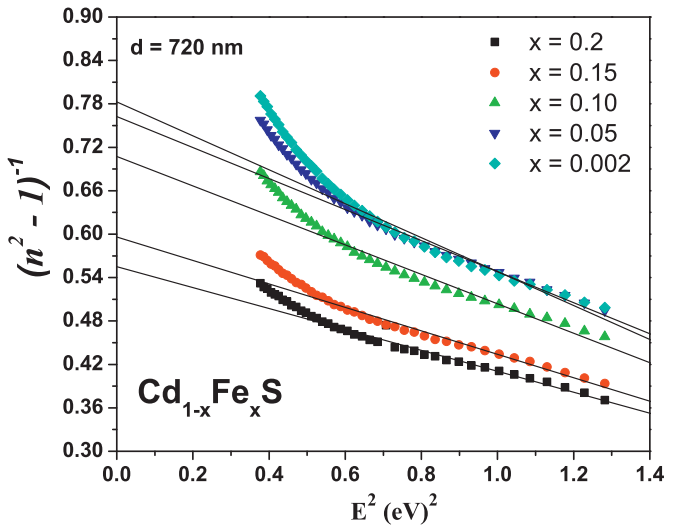

Fig. 6. The optical dispersion behavior, $(n^2-1)^{-1}$ against $(h\nu)^2$, of the investigated nanocrystalline $Cd_{1-x}Fe_xS$ thin films with different Fe content.

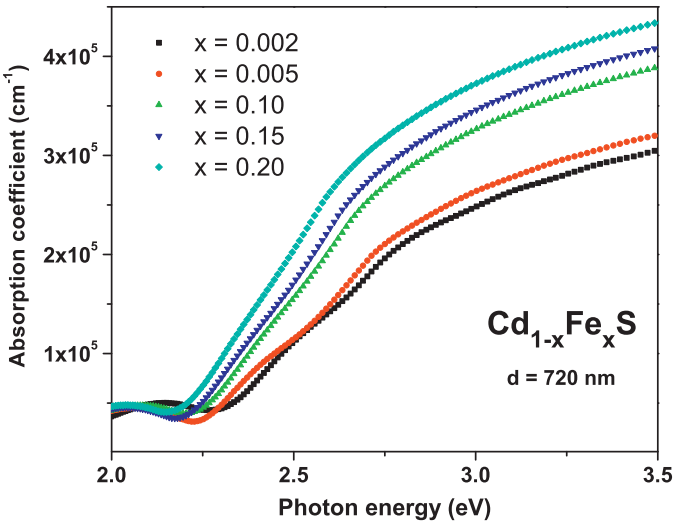

Fig. 7. The variation of the absorption coefficient $\alpha(\lambda)$ as a function of Fe content of nanocrystalline $Cd_{1-x}Fe_xS$ thin films.

energy with composition may be attributed to the observed shift of the optical transmission spectra in the short wavelength region, which shifts the absorption edge towards lower energies. However, the increase in the dispersion energy with x can be understood as arising mainly from the changes occurred in the effective number of electrons per anion N_e.

Further analysis of the $(n^2-1)^{-1}$ against $(h\nu)^2$ allows to determine the static refractive index, $n_0=(1+E_d/E_0)^{0.5}$, by extrapolating the WDD dispersion relation to the value of the incident photon energy $h\nu$ approaching zero. Moreover, the values of zero-frequency dielectric constant $\varepsilon_0=n_0^2$ were evaluated. The calculated values of the static refractive index n_0 and the zero frequency dielectric constant ε_0 for all the investigated films are listed in Table 2. It was observed that both the static refractive index and the zero frequency dielectric constant vary with the Fe content. Similar behavior for the variation of n_0 with the Mn concentration in $Zn_{1-x}Mn_xS$ system has been reported [25].

The refractive index n can also be further analyzed to determine the average interband oscillator wavelength (λ_0) and the average oscillator strength (S_0) for all investigated films with different Fe content by using the following single Sellmeier oscillator at low energies [26]

$$\frac{n_0^2-1}{n^2-1}=1-\left(\frac{\lambda_0}{\lambda}\right)^2 \tag{10}$$

Further, Eq. (10) also can be transformed as

$$n^2-1=\frac{S_0\lambda_0^2}{1-(\lambda_0/\lambda)^2} \tag{11}$$

The parameters, n_0 and λ_0 values were obtained from the slope and intercept of $(n^2-1)^{-1}$ vs. λ^{-2} curves (not shown).

The S_0 values for different Fe doped films were obtained using $S_0=(n_0^2-1)/\lambda_0^2$. The values of n_0, λ_0 and S_0 are summarized in Table 2.

3.3.3. Absorption coefficient and optical energy band gap analysis

The optical absorption coefficient, α, of as grown $Cd_{1-x}Fe_xS$ films with different composition ($0.002\le x\le 0.2$) is evaluated from the experimental data of transmittance and reflectance through the film/glass layered structure. At photon energies where the high absorption coefficient permits interference effects to be neglected, but not multiple internal reflections, the optical absorption coefficient is given as [27]:

$$\alpha(\lambda)=\left(\frac{1}{d}\right)\ln(A\times B) \tag{12}$$

$$A=\frac{(1-R_1)(1-R_2)(1-R_3)}{2T(1-R_2R_3)}, \tag{13}$$

and

$$B=1+\left\{\frac{1+[R_1(R_2+R_3-2R_2R_3)]}{(1-R_2R_3)A^2}\right\}^{1/2} \tag{14}$$

where T is the transmittance, R_1, R_2, R_3 are the power reflection coefficients of air/$Cd_{1-x}Fe_xS$ film, $Cd_{1-x}Fe_xS$ film/glass substrate and glass substrate/air interfaces, respectively and d is the thickness. Similarly, this method has been used for calculating the optical absorption coefficient of GaN films by Muth et al. [28] and mixed rare earth oxide $(Y_{1-x}Er_x)_2O_3$ by El-Hagary et al. [11]. Fig. 7 shows the variation of the absorption coefficient (α) with photon energy as a function of Fe content of nanocrystalline $Cd_{1-x}Fe_xS$ thin films. As shown in this figure the absorption coefficient increases with increasing Fe content. The optical energy band gap, E_g, of the nanocrystalline $Cd_{1-x}Fe_xS$ ($0.002\le x\le 0.21$) films can be determined from optical measurements in semiconductors by fitting the data to the Tauc's relation [24]:

$$(\alpha h\nu)^{1/\delta}=\alpha_0(h\nu-E_g) \tag{15}$$

Table 2
The optical parameters of the investigated nanocryatalline thin films of $Cd_{1-x}Fe_xS$ with different compositions.

x	E_g^{opt} (eV)	$E_g^{opt(WDD)}$ (eV)	E_0 (eV)	E_d (eV)	N_e	n_0	ε_0	λ_0 (nm)	$S_0\times10^{13}$ (m^{-2})
0.002	2.48	2.470	4.940	6.1322	2.072	1.496	2.24	251.613	2.681
0.05	2.46	2.435	4.871	6.1423	2.075	1.503	2.26	255.207	2.589
0.10	2.42	2.414	4.828	6.8263	2.306	1.552	2.41	257.463	2.509
0.15	2.38	2.404	4.807	8.1733	2.761	1.643	2.70	258.562	2.467
0.20	2.35	2.338	4.676	8.8990	3.006	1.702	2.90	265.800	2.312

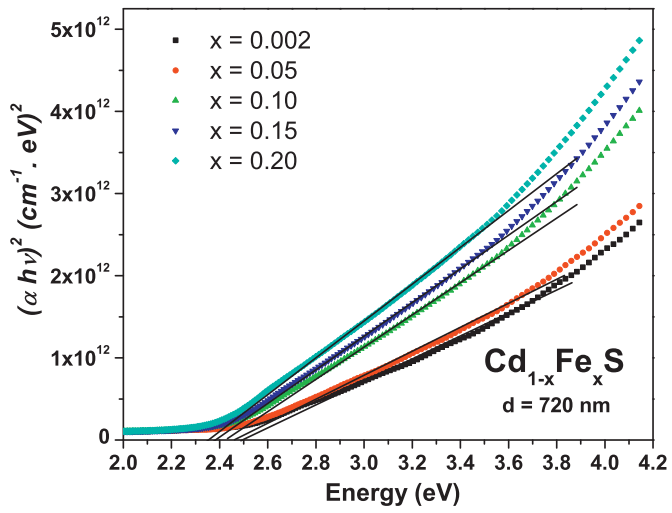

Fig. 8. Plot of $(\alpha h\nu)^2$ with the photon energy, $h\nu$, for as-deposited nanocrystalline $Cd_{1-x}Fe_xS$ ($x = 0.002$, 0.05, 0.1, 0.15 and 0.2) films.

where α_0 is a constant and δ is an exponent that depends on the type of the band transitions involved; e.g. $\delta = 1/2$ or 3/2 for allowed direct interband transitions and forbidden direct interband transitions, respectively. The direct band gap value of the as-deposited nanocrystalline $Cd_{1-x}Fe_xS$ ($0.002 \leq x \leq 0.2$) films is determined by extrapolating the straight portion to zero absorption. Fig. 8 shows the change of $(\alpha h\nu)^2$ as a function of $h\nu$ for nanocrystalline $Cd_{1-x}Fe_xS$ films. The obtained data were given in Table 2. It was found that the optical energy gap of the nanocrystalline $Cd_{1-x}Fe_xS$ films decreases with increasing of the Fe content. Similar behavior of the variation of the optical band gap with different Fe concentrations has been reported by other group [10]. The decrease in the band gap with increasing of the Fe content is suggested to be related to the *sp–d* exchange interaction with the Fe^{2+} magnetic moments. Presence of localized magnetic ions in semiconductors leads to exchange interaction between *s–p* band electrons and the Fe^{2+} electrons (*sp–d* exchange interaction). Similar behavior has been reported by different groups for $Zn_{1-x}Mn_xS$ system [25,29].

4. Conclusions

In conclusion, nanocrystalline thin films of CdS doped with Fe^{2+} ions with different doping concentrations ($x = 0.002$, 0.05, 0.1, 0.15 and 0.2) were prepared by electron beam evaporation technique. The lattice parameter was found to decrease with respect to Fe doping concentration and it exhibits cubic type structure. Grain size varies from 33 to 20 nm with the increase of Fe content. The optical properties were studied from their reflectance and transmittance in the spectral region. The refractive index and extinction coefficient have been found to increase with increasing Fe content. The increase in the refractive index with Fe content has been explained in terms of the polarizability. The dispersion of the refractive index is investigated using the WDD single oscillator model. The oscillator parameters were calculated. The optical energy gap has been estimated using the Tauc's method. The optical energy gap has been found to decrease from 2.48 for $x = 0.002$–2.35 for $x = 0.2$ which is explained on the basis of the *sp–d* exchange interaction with the Fe^{2+} magnetic moments.

Acknowledgement

This work was supported by the Deanship of the Scientific Research at Qassim University, Kingdom of Saudi Arabia in the framework of the Long-Term comprehensive National Plan for science, technology and innovation, under grant no. 09-ENV792-09.

References

[1] Diluted magnetic semiconductors, in: J.K. Furdyna, J. Kossut (Eds.), Semiconductors and Semimetals, vol. 25, Academic Press, London, 1988.
[2] J. Kossut, W. Dobrowolski, in: K.H.J. Buschow (Ed.), Magnetic Materials, vol. 7, North-Holland, Amsterdam, 1993, p. 231.
[3] R.L. Agarwal, J.K. Furdyna, S. Vonmolnar, DMS MRS. Sym. Proc. 89 MRS, Pittsburgh, 1987.
[4] A. Mycielski, J. Mycielski, J. Phys. Soc. Jpn. 49 (1980) 809.
[5] R.R. Galazaka, Inst. Phys. Conf. Ser. 43 (1979) 133.
[6] P.K. Willardson, A.C. Beer (Eds.), Semimetals and Semiconductors, vol. 25, Academic Press, New York, 1988.
[7] A. Twardowski, J. Appl. Phys. 67 (1990) 5108.
[8] A. Twardowski, P. Glod, W.J. Mdejonge, M. Demianiuk, Solid State Commun. 64 (1987) 63.
[9] S.J. Han, J.W. Song, C.H. Yang, S.H. Park, J.H. Jeong, Appl. Phys. Lett. 81 (2002) 4212.
[10] X.J. Wu, D.Z. Shen, Z.Z. Zhang, K.W. Liu, B.H. Li, J.Y. Zhang, Y.M. Lu, D.X. Zhao, B. Yao, X.G. Ren, X.W. Fan, Solid State Commun. 141 (2007) 344.
[11] M. El-Hagary, M. Emam-Ismail, S.H. Mohamed, A.S. Hamid, S. Althoyaib, Thin Solid Films 518 (2010) 4058.
[12] E.R. Shaaban, M. El-Hagary, M. Emam-Ismail, M.B. El-den, Philos. Mag. 91 (2011) 1679.
[13] D. Sreekantha Reddy, K. Narasimha Rao, K.R. Gunasekhar, N. Koteeswara Reddy, K. Siva Kumar, P. Sreedhara Reddy, Mater. Res. Bull. 43 (2008) 3245.
[14] I.O. Oladejia, L. Chow, J.R. Liu, W.K. Chu, A.N.P. Bustamante, C. Fredricksen, A.F. Schulte, Thin Solid Films 359 (2000) 154.
[15] B.D. Cullity, Elements of X-ray Diffraction, 2nd ed., Addition-Wesley, London, 1978.
[16] G.B. Williamson, R.C. Smallman, Philos. Mag. 1 (1956) 34.
[17] L.A. Agiev, I.N. Shklyarevskii, J. Prekel Spekt. 76 (1978) 380.
[18] I.N. Shklyarevski, T.I. Kornveeva, K.N. Zozula, Opt. Spectrosc. 27 (1969) 174.
[19] O.S. Heavens, Optical Properties of Thin Films, Dover, New York, 1965.
[20] S. Tolansky, Multiple-Beam Interference Microscopy of Metals, vol. 55, Academic Press, London, 1970.
[21] S.R. Elliott, The Physics and Chemistry of Solids, Wiley, Chichester, 2000.
[22] S.H. Wemple, DiDomenico, Phys. Rev. B 3 (1971) 1338.
[23] T. Tanaka, Thin Solid Films 66 (1980) 271.
[24] J. Tauc, Amorphous and Liquid Semiconductor, Plenum, New York, 1974.
[25] M. El-Hagary, M. Emam-Ismail, E. R. Shaaban, S., Althoyaib, Mater. Chem. Phys., doi:10.1016/j.matchemphys.2011.11.072, in press.
[26] A.K. Walton, T.S. Moss, Proc. Phys. Soc. 81 (1963) 509.
[27] S.H. Wemple, J.A. Seman, Appl. Opt. 12 (1973) 2947.
[28] J.F. Muth, J.H. Lee, I.K. Shmagin, R.M. Kolbas, H.C. Casey Jr., B.P. Keller, U.K. Mishra, S.P. DenBaars, Appl. Phys. Lett. 71 (1997) 2572.
[29] P.k. Ghosh, S.K.F. Ahmed, S. Jana, K.K. Chattopadhyay, Opt. Mater. 29 (2007) 1768.